

Shapes, sizes and light scattering properties of ice crystals in cirrus and a persistent contrail during SUCCESS

R. Paul Lawson
SPEC, Inc., Boulder, Colorado 80301

Andrew J. Heymsfield and Steven M. Aulenchbach
National Center for Atmospheric Research, Boulder, Colorado 80307

Tara L. Jensen
SPEC, Inc., Boulder, Colorado 80301

Abstract. A persistent contrail in the shape of a racetrack was generated by the NASA DC-8 research aircraft during the SUCCESS project. The contrail was visible on GOES imagery for six hours. Microphysical measurements collected by the DC-8 show that after 40 min the core of the contrail contained mostly small (1 to 20 μm) ice particles in concentrations $>1000 \text{ L}^{-1}$, with larger ($>300 \mu\text{m}$) ice crystals in concentrations $<10^4 \text{ L}^{-1}$. In contrast to the core, the contrail periphery contained about an order of magnitude less ice particles in the 1 \rightarrow 20 μm range and about three orders of magnitude more ice particles $>300 \mu\text{m}$. The larger ice crystals in the periphery were mostly columns and bullet rosettes, similar to habits of larger ice crystals found in ambient cirrus in the area. Measurements suggest that the shape of phase functions of randomly-oriented columns and rosettes are mostly featureless. The measured phase functions are closest in shape to those predicted by ray-tracing theory for random-fractal and spatial-dendrite ice crystals.

1. Introduction

A persistent contrail was formed by the NASA DC-8 research aircraft at about 11 km (-55°C) offshore of San Francisco on 12 May 1996 during the Subsonic Aircraft: Contrail and Cloud Effects Special Study (SUCCESS) project. Heymsfield et al. (1997) (in this issue) show the racetrack-shaped flight track of the DC-8 and the resulting contrail, along with measurements of lidar backscatter, relative humidity, particle concentration and size. The persistent contrail, with its distinctive racetrack pattern, was visible on GOES satellite imagery for about six hours while it moved eastward over the California mainland and dissipated in the lee of the Sierra Nevada mountains. Precipitation streamers, visible from the bottom of the contrail, were occasionally noted by the pilots on the DC-8.

In situ measurements from Heymsfield et al. (1997) show that, in the ambient environment and at the periphery of the contrail, the vapor content of the air was typically 20 - 40% supersaturated with respect to ice. On the other hand, the core of the contrail was at vapor saturation, the excess vapor being depleted by small ($<20 \mu\text{m}$) particles in concentrations of about 1 to 10 cm^{-3} . The measurements suggest that a turbulent process results in a small percentage of the particles being mixed from the core into the vapor-rich environment at the periphery of the contrail, where they

grow to sizes $>300 \mu\text{m}$ and may form virga (i.e., precipitation streamers). The in situ measurements are in general agreement with earlier work by Knollenberg (1972) and Heymsfield (1973).

Persistent contrails have been observed to coalesce into clouds which take on the appearance of cirrus and can act to measurably reduce the incoming solar radiation in heavily trafficked flight corridors of Europe and elsewhere (Bakan et al. 1994). The light-scattering properties of ice crystals and radiative characteristics of cirrus clouds are strongly dependent on particle shape (Mishchenko et al. 1996a). A new in situ sensor, which was installed for the first time on the DC-8, provided high-resolution (5 μm) digital images of the ice particles. The instrument, called a particle imaging nephelometer, or Π -Nephelometer, simultaneously records the particle image and measures the scattering phase function of the imaged particle. The shapes of ice particles with images $>50 \mu\text{m}$ are readily discernible and provide information of typical particle shapes in the periphery of the contrail and in cirrus which occurred naturally in the vicinity of the contrail. Measurements collected in the Colorado State University (CSU) dynamic cloud chamber (DeMott et al. 1990) after the SUCCESS project were used to correlate the imaged particles with the scattering phase function.

The measurements on 12 May 1996 show that the size distributions of particles within the core of the contrail differ from those on the periphery, in the precipitation streamers and in the ambient cirrus. Consequently, the light-scattering properties of these regions can be expected to differ, which in turn influences their optical and radiative characteristics.

2. Instrumentation

The NASA DC-8 was extensively instrumented for microphysical research. In addition to the Π -Nephelometer, microphysical measurements from instruments discussed in this paper include:

(1) A multi-angle aerosol spectrometer probe (MASP), described by Baumgardner et al. (1996), measures particle size distribution in the range from 0.3 - 40 μm ;

(2) a video ice particle sampler (VIPS), as described by Heymsfield and McFarquhar (1996), uses 30 Hz video images to estimate the particle size spectra for particles of at least 5 μm diameter. During this flight, there was a focusing problem which limited the minimum detectable size to 30 μm ; and

(3) a PMS 2D-C probe (Knollenberg 1981) with a lower detection threshold of between 50 and 100 μm .

The Π -Nephelometer casts an image of a particle on a 400,000 pixel solid-state camera by freezing the motion of the particle using a 25 ns pulsed, high-power (60 W) laser diode. Unique op-

Copyright 1998 by the American Geophysical Union.

Paper number 98GL00241.
0094-8534/98/98GL-00241\$05.00

tical imaging and particle detection systems (PDS) precisely detect particles and define the depth-of-field (DOF) so that at least one particle in the image is almost *always in focus*. This eliminates out-of-focus sizing errors that have plagued the conventional 2D imaging probes (Korolev et al. 1991, 1998).

The II-Nephelometer was designed to record up to 25 frames s^{-1} , although a software bug prevented the instrument from recording more than 5 frames s^{-1} . This severely limited the imaging sample volume.¹ However, the particle detection system was always active and recorded the number of particles $> 20 \mu m$ which traversed the 3 mm by 4 mm particle detection area. At 225 $m s^{-1}$, the sample volume of the PDS is 2.8 $L s^{-1}$. Particle size distributions were computed by averaging several seconds of image data and scaling the concentration using measurements from the PDS.

The scattered light system (SLS) consists of twenty-eight 1-mm optical fibers connected to microlenses bonded on the surface of avalanche photo diodes (APDs). The fibers are placed at discrete angles of 11, 20, 28, 37, 45, 53, 61, 70, 110, 118, 127, 135, 143, 152 and 160°. The field of view of each fiber is about $\pm 2^\circ$, except for the 11° fiber which integrates forward scattered light from about $3.5 \rightarrow 18^\circ$.

3. Size distributions and shapes of ice crystals

Heymsfield et al. (1998) show five DC-8 racetrack-shaped flight patterns on 12 May 1996 which often overlap and sometimes intersect ambient cirrus clouds which were scattered over the area. The ambient cirrus and overlapping contrails confounded unique determination of the origin of the ice particles. The central cores of the contrails were often detectable from distinctly elevated NO_x concentrations (Weinheimer et al. 1997). The peripheries of the contrails were delineated on either side of the central core. The contrails and precipitation streamers were occasionally visible from the cockpit of the DC-8, and intercom voice notes were used to determine the position of the aircraft relative to the visible contrail. Lidar observations, shown in Heymsfield et al. (1998), were also used to identify cirrus that was above or below the aircraft. These composite observations were used to select representative regions of the contrail core, periphery and ambient cirrus.

Ambient cirrus. The cirrus clouds in the area near the contrail were mostly thin, patchy and contained occasional particles up to 1 mm in maximum dimension. Fig. 1 shows a combined particle size distribution using the MASP, VIPS, II-Nephelometer and 2D-C probes along with examples of images of particles observed by the II-Nephelometer from 225230 - 225630 GMT. There is good general agreement in the shapes of the particle size distributions measured by the VIPS, II-Nephelometer and 2D-C probes for particles from about 75 - 500 μm . In Fig. 1, the columns extend to about 200 μm in length and the maximum dimensions of bullet rosettes are up to 600 μm . The shape of the smallest ($< 50 \mu m$) particles often cannot be determined. They usually appear to be mostly spheroidal in shape, however, this may be due to the II-Nephelometer 5 μm pixel resolution, which is not always adequate to resolve the edges of plates $< 50 \mu m$. As a result, in this paper we have elected to classify small particles that appear spherical in shape as "unresolved spherical". The shape of particles from 50 to 200 μm are mostly columnar and/or rosettes, and particles $> 200 \mu m$ are usually bullet rosettes.

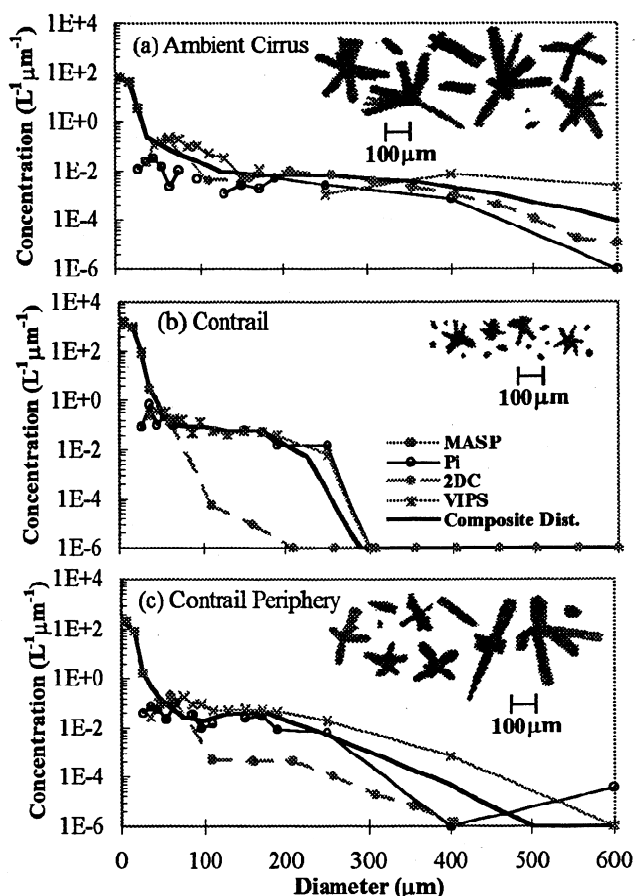


Figure 1. Particle size distributions from the MASP, VIPS, II-Nephelometer (Pi), 2D-C measurements and composite distribution in (a) ambient cirrus, (b) contrail core and (c) contrail periphery. Examples of images from the II-Nephelometer are shown next to each case.

Contrail cores. The central cores of contrails typically contain high concentrations of small ice particles (Knollenberg 1972; Heymsfield et al. 1998). A contrail core, identified by $NO_x > 100$ ppt was sampled from 233938 to 233952 (Heymsfield et al. 1998). The composite size distribution shown in Fig. 1 is dominated by the small particles seen by the MASP. Images of the small particles recorded by the II-Nephelometer were classified as "unresolved spherical". High-resolution replicas seen on the Desert Research Institute (DRI) home page (<http://www.dri.edu>) suggest that particles $< 20 \mu m$ in contrails are often plates and columns, combined with irregular and spheroidal shapes. However, the crystals seen on the DRI home page were all observed in an environment with low ($< 100\%$) relative humidity and may not be representative of the 12 May contrail, which was typified by very high relative humidity. More than 99% of the ice particles in the core of the 12 May contrail were $< 20 \mu m$ and the low concentration of 100 to 250 μm rosettes may have mixed in from the contrail periphery (Heymsfield et al. 1998).

Contrail periphery and precipitation streamers.

Heymsfield et al. (1998) show data from a penetration of a contrail that was about 40 min old. The DC-8 penetrated the contrail downward from above. Data from the lidar suggested that the contrail itself was not contaminated from cirrus aloft and that there were some regions that contained precipitation streamers. Heymsfield et al. (1998) show MASP measurements of total concentration of particles from about 1 to 10 μm in the contrail

¹ Upgrades after completion of the SUCCESS project included a 1 million pixel CCD camera, 2.3 μm pixel resolution, increased optical contrast and 40 frames s^{-1} data recording rate (see Lawson et al. 1998).

periphery that are 1 to 2 orders of magnitude lower than in the core. The composite particle size distribution and Π -Nephelometer images shown in Fig. 1 suggest that the contrail periphery contains particle types that are very similar to ambient cirrus, with the exceptions that there are additional small particles and fewer particles in the 300–600 μm range. Heymsfield et al. (1998) suggest that a turbulent process occurs whereby some particles in the core are mixed into the vapor-rich region of the periphery and grow to larger sizes.

As the DC-8 continued its descent, it may have also penetrated precipitation streamers below the contrail; however, some of the regions also contained ambient cirrus and separating the two was unambiguous. Basically, the data suggest that the particles continued to grow in the vapor-rich environment as they precipitated from the contrail, sometimes reaching sizes up to about 1 mm. The habits of particles in the precipitation streamers appeared to be dominated by bullet rosettes.

4. Light scattering properties of the ice crystals

Calculations shown in Mishchenko et al. (1996a) suggest that using the wrong scattering phase function in retrieving cloud optical thickness can result in an overestimation or underestimation of optical thickness by more than a factor of three. The Π -Nephelometer was used to measure the phase functions of ice crystals in the CSU cloud chamber. Before the data collection, extensive laboratory tests were conducted with water drops and glass beads. Comparisons with Mie scattering theory for 20 to 200 μm water drops and Π -Nephelometer measurements were in good relative agreement. However, measurements of 50 and 100 μm glass beads scattered nearly an order of magnitude more light in the region from 80° to 120° than predicted by Mie theory for a spherical glass bead. Gayet (1997 - personal communication) observed a nearly identical departure from Mie theory in the 80° to 120° region when measuring phase functions from glass beads with a polar nephelometer (Gayet et al. 1997). Mishchenko et al. (1996b) found very similar results when comparing micron-size spheres with equivalent area spheroids and soil particles. This suggests that even minute degrees of non-sphericity can lead to large differences in phase functions.

Fig. 2 shows phase functions for 20 μm water drops generated in the laboratory and ice particles observed in the CSU cloud chamber along with examples of Π -Nephelometer images. All of the phase functions shown in Fig. 2 are normalized to the light intensity measured at the 20° scattering angle for a 20 μm water drop. The dynamic chamber was operated in a way such that a cloud was formed by an adiabatic expansion at about -20°C (540 mb), seeded at -28°C and ice crystals grew as the expansion continued to about -42°C (380 mb). The Π -Nephelometer images were sorted by size and the particle shapes observed in the 12 May contrail and ambient cirrus. Figure 2 shows that the relative intensities of the phase functions for small (20 to 50 μm) particles are strongly a function of particle shape. The data show that in the 20 to 50 μm (Sm.) size range, progressively more light is scattered (from about 40° → 160°) as the particle shape becomes more complex, from water drops → unresolved spheroids → irregulars → columns and rosettes. In Fig. 2, for the 50 to 90 μm (Med.) and 90 to 210 μm (Lg.) size ranges, it appears that the influence of particle shape on phase function decreases. For particles > 50 μm , the data suggest that size is the significant factor influencing the amount of light scattered.

Figure 2 also shows phase functions derived from ray-tracing for a dendrite (Takano and Liou 1995), a column and a fractal (Mishchenko et al. 1996a). The prominent 22° halo seen for the

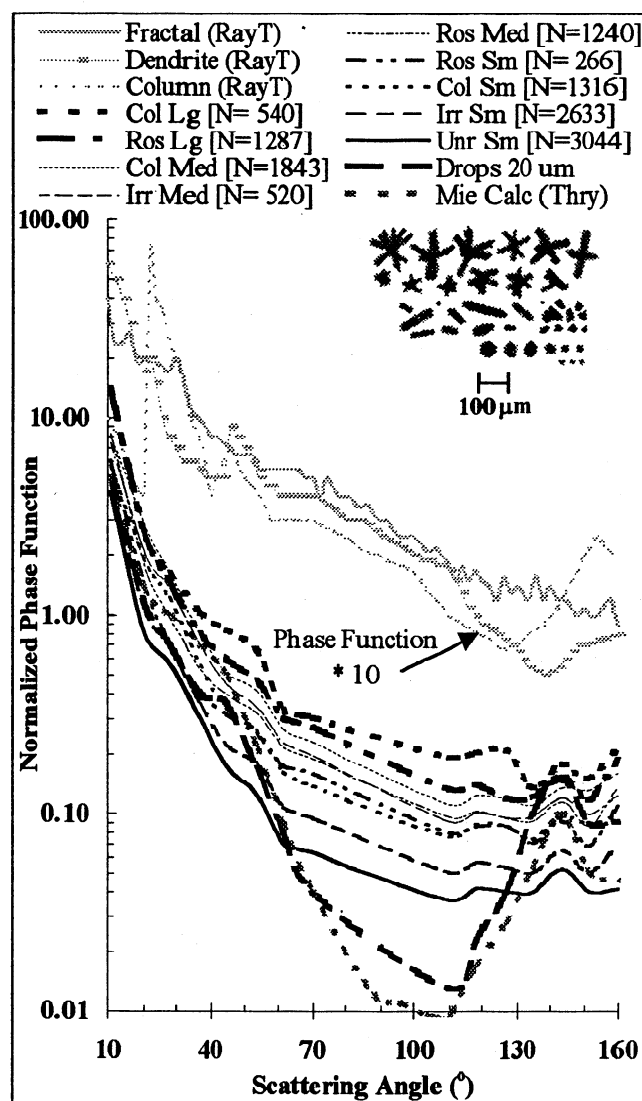


Figure 2. Normalized phase functions derived from measurements of ice crystals in the CSU cloud chamber compared with theory. Lighter lines offset by one decade toward the top of the figure are phase functions derived from ray-tracing for random-fractal and columnar crystals (Mishchenko et al. 1996) and a spatial dendrite (Takano and Liou 1995). Shown in lower part of figure (top to bottom) measurements from columns (Col), bullet rosettes (Ros), irregular shaped crystals (Irr), and unresolved spherical (Unr), 20 μm drops, and Mie Theory (Thry) for 20 μm drop. Size bins indicated in legend for measured crystals include 20–50 μm (Sm.), 50–90 μm (Med.), and 90–210 μm (Lg.). Number (N) of measurements for each crystal type is included in legend. Also, examples of Π -Nephelometer images of bullet rosettes (top row), columns and irregular shapes (middle row), and unresolved spherical crystals (bottom row) are shown in the middle right of the figure.

column is not observed in the measurements. Mostly, the measured phase functions are featureless with some suggestion of a peak near 145°. The best agreement between the measurements and ray-tracing theory appears to be with the fractal and dendritic crystals. Nikiforova et al. (1978) and Volkovitskiy et al. (1980) also made measurements in a cloud chamber. They used a “Rassvet” device (Nikiforova et al. 1978), which averaged meas-

urements over a range of discrete angles and a time period of 10 s. The phase functions shown by Nikiforova et al. (1978) do not display the 22° halo for the small ice crystals and the authors comment that the 22° halo was only observed in clouds with low optical density. Interestingly, Nikiforova et al. (1978) do show a slight bump at 145° for both ice and water clouds. Volkovitskiy et al. (1980) show a 22° halo in their measurements, although they comment that it is not nearly as prominent as predicted from ray-tracing. The principal difference between the measurements using the Rassvet device and the Π -Nephelometer, is that crystals are sucked through a 25 mm sample tube in a *random* orientation in the Π -Nephelometer, and they are allowed to fall undisturbed through the Rassvet device. Apparently, under conditions where the optical density is low and hexagonal crystals are allowed to fall naturally with the c-axis oriented vertically, the 22° halo is observed in the cloud chamber with the Rassvet device.

5. Discussion and summary

Measurements in the 12 May SUCCESS contrail show that the ice particles observed in the core were small, mostly 1 → 20 μm , and while they appeared spheroidal in shape, instrument resolution prevented determination of plates and similar shapes that may appear to be nearly spherical. On the contrail periphery, where the relative humidity exceeded ice saturation by 20–40%, ice particles as large as 300–500 μm were observed. Particle shapes in the periphery included unresolved spherical, irregular, columnar and bullet rosette. Ice crystals larger than about 200 μm were typically bullet rosettes. It is postulated (Heymsfield et al. 1998) that the larger crystals fall out of the contrail periphery and become precipitation streamers. The shapes of ice particles in the contrail periphery were typical of those sampled in patches of cirrus observed in the area; however, the cirrus contained fewer small particles and more larger ice crystals, extending to sizes of 600 μm and occasionally 1 mm.

The shapes and sizes of ice particles generated in the CSU cloud chamber were remarkably similar to those observed in the contrail and ambient cirrus. Measurements of phase functions in the cloud chamber suggest that for small randomly-oriented (< 50 μm) ice particles, as the crystal departs more from a spherical shape, relatively more light is scattered in the 40° → 160° region. Volkovitskiy et al. (1980) also found that more light is scattered from ice particles than cloud drops in this range of angles, and they suggest that this is due to relatively weaker scattering for ice particles in the 2 → 40° range. Our measurements suggest that light scattered in the 40° → 160° range from randomly-oriented ice crystals > 50 μm has a weaker dependence on crystal type and that crystal size is the dominant factor. Of course, these conclusions are based on a limited data set, about 12,000 individual ice crystals generated in a cloud chamber, and more data are needed for additional verification.

Acknowledgments. The authors wish to thank Dr. Greg McFarquhar for his help with VIPS and 2D-C data and Dr. Darrel Baumgardner for providing MASP data. We would also like to thank Dr. Tim Quakenbush and Dr. Paul DeMott for their assistance in obtaining the Π -Nephelometer data. We are grateful for suggestions made by two anonymous reviewers. Finally, Cheryl Hilliard is thanked for her help in the preparation of this manuscript. The SPEC, Inc. part of this study was supported by the following programs: NASA/SBIR NAS1-19591, NASA/SUCCESS NAS2-

14258 and NASA FIRE NAS1-96015. Grants to NCAR include: NASA/SUCCESS grant A49760D; NASA/FIRE-III grant L55549D and Air Force Office of Scientific Research grant F49620-96-C-0024.

References

- Bakan, S., M. Betancor, V. Gayler and H. Grassl, 1994: Contrail frequency over Europe from NOAA-satellite images. *Annal. Geophys. Atmos., Hydro. and Space Sci.*, 12, 962.
- Baumgardner, D., J. E. Dye, B. Gandrud, K. Barr, K. Kelly and R. K. Chan, 1996: Refractive indices of aerosols in the upper troposphere and lower stratosphere. *Geophys. Res. Lett.*, 23, 749–752.
- DeMott, P. J., D. C. Rogers and R. P. Lawson, 1990: Improvements to the CSU controlled-expansion cloud chamber. Preprints: ICCP Conference on Cloud Physics, San Francisco, 126–129.
- Gayet, J.-F., O. Cr  pel, J.-F. Fournol and S. Oshchepkov, 1997: A new airborne Polar Nephelometer for the measurements of optical and microphysical cloud properties. Part I: Theoretical design. *Annales Geophysicae*, 15, 451–459.
- Heymsfield, A. J., 1973: Laboratory and field observations of the growth of columnar and plate crystals from frozen droplets. *J. Atmos. Sci.*, 30, 1650–1656.
- Heymsfield, A. J. and G. M. McFarquhar, 1996: On the high albedos of anvil cirrus in the tropical Pacific warm pool: Microphysical interpretations from CEPEX and from Kwajalein, Marshall Islands. *J. Atmos. Sci.*, 53, 2424–2451.
- Heymsfield, A. J., R. P. Lawson and G. Sachse, 1998: Development of ice particles precipitating from a contrail during SUCCESS. In this issue of *Geophys. Res. Letter*.
- Knollenberg, R. G., 1972: Measurements of the growth of the ice budget in persisting contrail. *J. Atmos. Sci.*, 29, 1367–1374.
- Knollenberg, R. G., 1981: Techniques for probing cloud microstructure. *Clouds Their Formation, Optical Properties, and Effects*, P. V. Hobbs and A. Deepak, Eds., Academic Press, 15–91.
- Korolev, A. V., S. V. Kuznetsov, Y. E. Makarov, and V. S. Novikov, 1991: Evaluation of measurements of particle size and sample area from optical array probes. *J. Atmos. Oceanic Technol.*, 8, 514–522.
- Korolev, A. V., J. W. Strapp, and G. A. Isaac, 1998: On the accuracy of PMS optical array probes. To Appear: *J. Atmos. Oceanic Technol.*
- Lawson, R. P., A. V. Korolev, S. G. Cober, T. Huang, J. W. Strapp and G. A. Isaac, 1998: Improved Measurements of the Drop Size Distribution of a Freezing Drizzle Event. To Appear: *Atmos. Res.*
- Mishchenko, M. I., W. B. Rossow, A. Macke and A. A. Lacis, 1996a: Sensitivity of cirrus cloud albedo, bidirectional reflectance and optical thickness retrieval accuracy to ice particle shape. *J. Geophys. Res.*, 101, 973–985.
- Mishchenko, M. I., L. D. Travis and A. Macke, 1996b: Light scattering by nonspherical particles in the atmosphere: An overview. *IRS'96: Current Problems in Atmospheric Radiation*, W. L. Smith and K. Stamnes, eds., Deepak Publ.
- Nikiforova, N. K., L. N. Pavolova and V. P. Snykov, 1978: The "Rassvet" high-speed scattering phase function measuring system. *Trudy. IEM*, 83, 28–32.
- Takano, Y. and K. N. Liou, 1995: Radiative transfer in cirrus clouds; Part III: Light scattering by irregular ice crystals. *J. Atmos. Sci.*, 52, 818–837.
- Volkovitskiy, O. A., L. N. Pavlova and A. G. Petrushin, 1980: Scattering of light by ice crystals. *Izvestiya, Atmos. Oceanic Phys.*, 16, 98–102.
- Weinheimer, A. J., D. Baumgardner, T. L. Campos, F. E. Grahek, B. Gandrud, E. J. Jensen, B. A. Ridley, C. H. Twohy and J. G. Walega, 1997: Uptake of NO_y on wave-cloud ice particles. In this issue of *Geophys. Res. Lett.*

T. Jensen and R. P. Lawson, SPEC, Inc., 5401 Western Avenue, Suite B, Boulder, Colorado 80301. (email: plawson@specinc.com; jensen@specinc.com)

S. Aulenbach and A. Heymsfield, National Center for Atmospheric Research, P.O. Box 3000, Boulder, Colorado 80307.

(Received August 22, 1997; revised January 16, 1998; accepted January 20, 1998.)